Article

Aerobic Oxidation of Alcohols Catalyzed by In Situ Generated Gold Nanoparticles inside the Channels of Periodic Mesoporous Organosilica with Ionic Liquid Framework

Babak Karimi, Akram Bigdeli, Ali Asghar Safari, Mojtaba Khorasani, Hojatollah Vali, and Somaiyeh Khodadadi Karimvand

ACS Comb. Sci., **Just Accepted Manuscript** • DOI: 10.1021/acscombsci.9b00160 • Publication Date (Web): 16 Jan 2020

Aerobic Oxidation of Alcohols Catalyzed by *In Situ* Generated Gold Nanoparticles inside the Channels of Periodic Mesoporous Organosilica with Ionic Liquid Framework

Babak Karimi†‡, Akram Bigdeli†, Ali Asghar Safari†, Mojtaba Khorasani†‡, Hojatollah Vali§ and Somaiyeh Khodadadi Karimvand†*

† Institute for Advanced Studies in Basic Sciences, No. 444, Prof. Sobouti Boulevard, P.O. Box 45195-1159, Zanjan 45137-66731, Iran.

‡ Research Center for Basic Sciences & Modern Technologies (RBST), Institute for Advanced Studies in Basic Sciences (IASBS), Prof. Sobouti Boulevard, Zanjan 45137-66731, Iran.

§ Department of Anatomy and Cell Biology and Facility for Electron Microscopy Research, McGill University, Montreal, Quebec H3A 2A7, Canada.

KEYWORDS: Periodic Mesoporous Organosilica (PMO), Au Nanoparticles, Alcohol Oxidation, Heterogeneous Catalyst, Ionic Liquid.

Abstract

In situ generated gold nanoparticles inside the nanospaces of periodic mesoporous organosilica with imidazolium framework (Au@PMO-IL) were found to be a highly active, selective and reusable catalyst for the aerobic oxidation of activated and non-activated alcohols under mild reaction conditions. The catalyst was characterized by nitrogen adsorption-desorption measurement, thermogravimetric analysis (TGA), transmission electron microscopy (TEM), elemental analysis (EA), diffuse reflectance infrared Fourier transform spectroscopy (DRIFT), X-ray photoelectron spectroscopy (XPS) and inductively coupled plasma atomic emission spectroscopy (ICP-AES). The catalyst exhibited excellent catalytic activity in the presence of either Cs_2CO_3 (35 °C) or K_2CO_3 (60 °C) as reaction bases in toluene as a reaction solvent. Under both reaction conditions, various types of alcohols (up to 35 examples) including activated benzylic, primary and secondary aliphatic, heterocyclic and challenging cyclic aliphatic alcohols

converted to the expected carbonyl compounds in good to excellent yields and selectivity. The catalyst also recovered and reused at least for seven reaction cycles. Data from three independent leaching tests indicated that amounts of leached gold particles were negligible (< 0.2 ppm). It is believed that the combination of bridged imidazolium groups and confined nanospaces of PMO-IL might be major reason explaining remarkable stabilization and homogeneous distribution of in-situ generated gold nanoparticles, thus resulting in the highly active and recyclable catalyst system.

Introduction

Selective oxidation of alcohols to the related carbonyl compounds such as aldehydes, ketones and carboxylic acids, considered as one of the most interesting research topics since desired products are extensively used in the synthesis of pharmaceuticals, agricultural and fine chemicals.[1] These transformations have been traditionally performed by using stoichiometric amounts of harmful organic as well as inorganic oxidants. Therefore, during recent two decades, in viewpoints of green chemistry and specially atom economy, a plethora of researches have been directed toward the development of new and efficient catalytic systems on the basis of molecular oxygen or hydrogen peroxide as green terminal oxidants.[2] In this regard, many sophisticated protocols based on transition-metal catalyst were developed in either homogeneous or heterogeneous form. However, for many practical applications heterogeneous compared to homogeneous catalysis stands with greater promise because of simple recovery of the catalyst as well as minimization of metal contamination in the final products.[3-7]

Various supported metal catalysts on the basis of gold, palladium, platinum, and ruthenium and etc. in the form of metal nanoparticles (NPs) has thus far been employed in the liquid phase aerobic oxidation of alcohols.[8-18] Not only these systems provide the advantages of recovering and reusing

the catalysts, but it has been demonstrated that synergistic effect between support and supported metal NPs may also improve the selectivity and life time of catalyst.[19-42] Among several metal catalysts reported so far, gold catalysts have received particular attentions due to their excellent performance in the aerobic oxidation of alcohols under ambient conditions.

Similar to other noble metals, nano and sub-nano gold particles have shown very interesting activities, selectivities as well as turn over numbers in the variety of catalytic processes.[43] In this context, it has been well documented that the activity, selectivity and life time of the gold nanoparticles depend not only on size and shape of the particles, but it can be significantly influenced by the nature of support, location of gold on the support, and synergistic interactions between gold and supporting materials.[44] In order to prevent the agglomeration of Au nanoparticles and retain high catalytic activity, several stabilizing agents such as poly-vinylpyrrolidone (PVP), sugars, surfactants, and various types of solid supports have been used during the synthesis steps and/or when they acted in desired reaction mediums.[45-46] Although, considerable improvements have been achieved in the catalytic activity, selectivity and substrate scope, there are still major problems with Au nanoparticle based catalysts. Primarily, the control in size of Au nanoparticles is a highly challenging because of very low melting point of gold.[47-48] Recently, we reported the preparation of Au nanoparticles on a bifunctional phenylene/ethylene periodic mesoporous organosilica (Au@PMO).[49] The catalyst was then successfully employed in the aerobic oxidation of alcohols under ambient temperature. Meanwhile we discovered that incorporating an appropriate concentration of bridged imidazolium group inside the framework of mesoporous silica led to innovative functional materials (so called PMO-IL) which serve as superior supported ionic liquid and/or effective support for immobilization and stabilization of metal nanoparticles in several synthetically important transformations.[50-57] It was demonstrated that in these materials the

molecular diversity of IL-like nanostructures that act as effective solid ionic stabilizer for metal nanoparticles is genuinely combined with the advantages of an integrated reaction and purification strategy. In particular, by using XPS studies we showed that Au supported on PMO-IL (Au@PMO-IL) in the form of Au(III) species is an efficient catalyst in the A^3-coupling reaction of aldehyde with amine and phenylacetylen to give the corresponding propargylamines.[58] Considering the excellent capability of PMO-IL in immobilization and stabilization of metal nanoclusters, in our present work, we attempt to explore the use of Au@PMO-IL in the aerobic oxidation of alcohols under mild reaction conditions. With this goal in mind, the aerobic oxidation of several alcohols was investigated for confirming the general applicability of Au@PMO-IL catalyst in the presence of either Cs_2CO_3 (at room temperature) or K_2CO_3 (at 60-80 °C). The advantage of our catalyst systems relies on the fact that in contrary to most of the reported gold catalysts the pre-generation of gold nanoparticles by employing an exogenous reducing agent is not required. More importantly, the open pore structure of Au@PMO-IL not only exposes a highly catalytically active species, but it also combines the possibility of separating and recycling both ionic liquid and supported Au NPs at the same times, the features that are all together of paramount importance for heterogeneous catalysis.

Result and Discussion

The synthesis of bridged ionic liquid 1,3-bis(3-trimethoxysilylpropyl)-imidazolium chloride (BTMSPC) was accomplished according to our reported procedures with a few modification.[50] The PMO-IL was then prepared using hydrolysis and co-polymerization of both BTMSPCl and tetramethoxyorthosilicate (TMOS) in the presence of Pluronic P123 as effective structure directing agent (SDA) under acidic conditions.[50] Surfactant was then removed by acidic ethanol to provide

PMO-IL. The resulting PMO-IL was then used to immobilize anionic gold species ($AuCl_4^-$) via a simple ion-exchange-impregnation technique according to our previous reported procedure with slight changes.[58] In this regard, PMO-IL was first sonicated in water to obtain a homogeneous distribution of particles of materials and then a solution of $NaAuCl_4$ was added to replace some of PMO-IL chloride counter ions with $AuCl_4^-$ until the final catalyst which is denoted as Au@PMO-IL was obtained.

The textural and structural feature of PMO scaffold and Au@PMO-IL were evaluated by nitrogen sorption analysis. Figure 1 displays N_2 adsorption–desorption isotherms and BJH pore size distributions (inset) for all materials. N_2 adsorption–desorption isotherms exhibit type IV adsorption isotherms with H1 hysteresis loops which are characteristics of mesoporous materials with narrow pore size distributions.[59] As evidenced by these investigations, the shape of isotherm in Au@PMO-IL is well-retained as compared with that of pristine PMO-IL, suggesting that the structure ordering survived during the mere ion-exchange process. Moreover, narrow pore size distributions for both PMO-IL and Au@PMO-IL indicate high-ordered structure in the mentioned materials (Figure 1, inset). The textural parameters of PMO-IL, fresh Au@PMO-IL and recovered catalyst are summarized in Table 1. These results show that after immobilization of the anionic $AuCl_4^-$ species into the PMO-IL channels, the specific surface area, total pore volume, and average pore diameter decreased from initial amounts of 530 $m^2\ g^{-1}$, 0.99 cm3 g-1 and 10.6 nm to 432 $m^2\ g^{-1}$, 0.77 $cm^3\ g^{-1}$ and 9.2 nm, respectively. On the basis of these measurements, the incorporation of $AuCl_4^-$ species shows minor effects on the pore size, pore volume and surface area. While the decrease in nitrogen uptake under the relative pressure 0.6-0.8 demonstrates successful immobilization of $AuCl_4^-$ ions inside the mesochannels of PMO-IL, the isotherms clearly reflect the excellent pore opening in the materials after ion-exchange process.

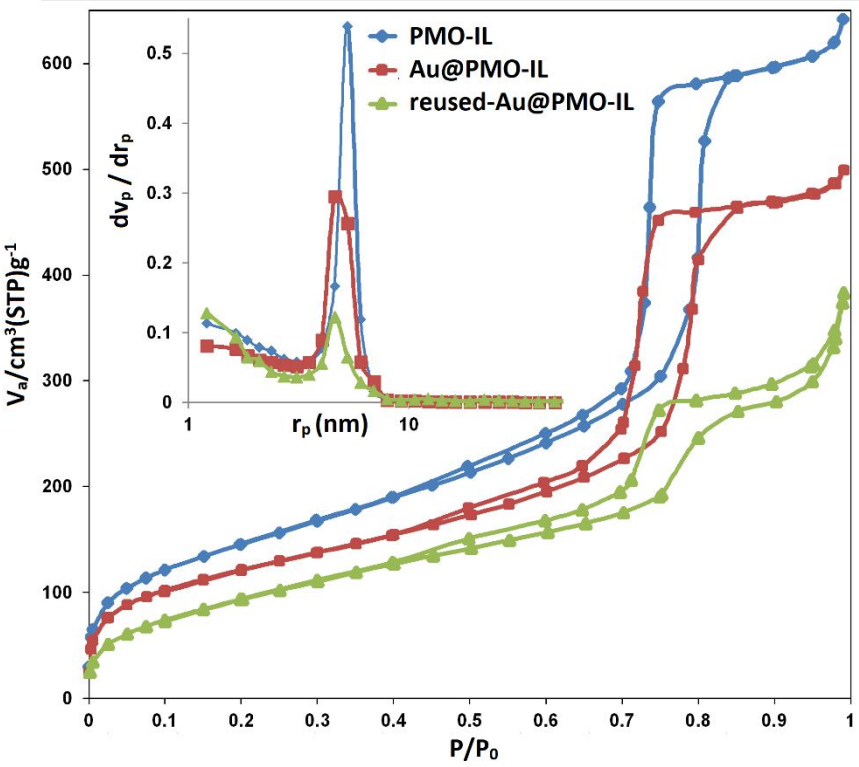

Figure 1. N_2 adsorption-desorption isotherms and BJH Pore size distributions (inset) for PMO-IL, Au@PMO-IL and recovered Au@PMO-IL.

Table1. Textural properties of the PMO-IL, Au@PMO-IL and recovered Au@PMO-IL.

Material	S_{BET}[a] (m^2g^{-1})	V_t[b] (cm^3g^{-1})	D_{BJH}[c] (nm)	F.G.[d] (mmol g^{-1})
PMO-IL	530	0.98	10.6	IL(1.1)
Au@PMO-IL	432	0.77	9.21	Au (0.090)
Recovered Au@PMO-IL	355	0.58	9.2	Au (0.085)

[a] S_{BET}: specific surface area from linear part of adsorbed nitrogen in the range from 0.05 to 0.3. [b] V_t: total pore volume derived from adsorbed nitrogen from relative pressure ≈ 0.99. [c] D_{BJH}: average pore size diameter calculated from the adsorption branch using BJH method. [d] Loading of functional groups estimated by TGA, elemental analysis or ICP-AES.

TEM studies were performed on PMO-IL and Au@PMO-IL, in order to confirm uniform mesoporous structure in the materials. TEM image of PMO-IL (Figure 2a) clearly demonstrates formation of a long-range ordered mesoporous structure with estimated pore size of 10 nm. On the other hand, TEM image of catalyst Au@PMO-IL also establishes that periodicity in the mesoporous structure is retained during catalyst preparation (Figure 2b). From this image it is clear that no formation of Au nanoparticles or aggregation was occurred either on the external surface or inside the mesochannels of PMO-IL. Overall, these finding are in good agreement with results obtained by N_2 adsorption-desorption analysis (Table 1).

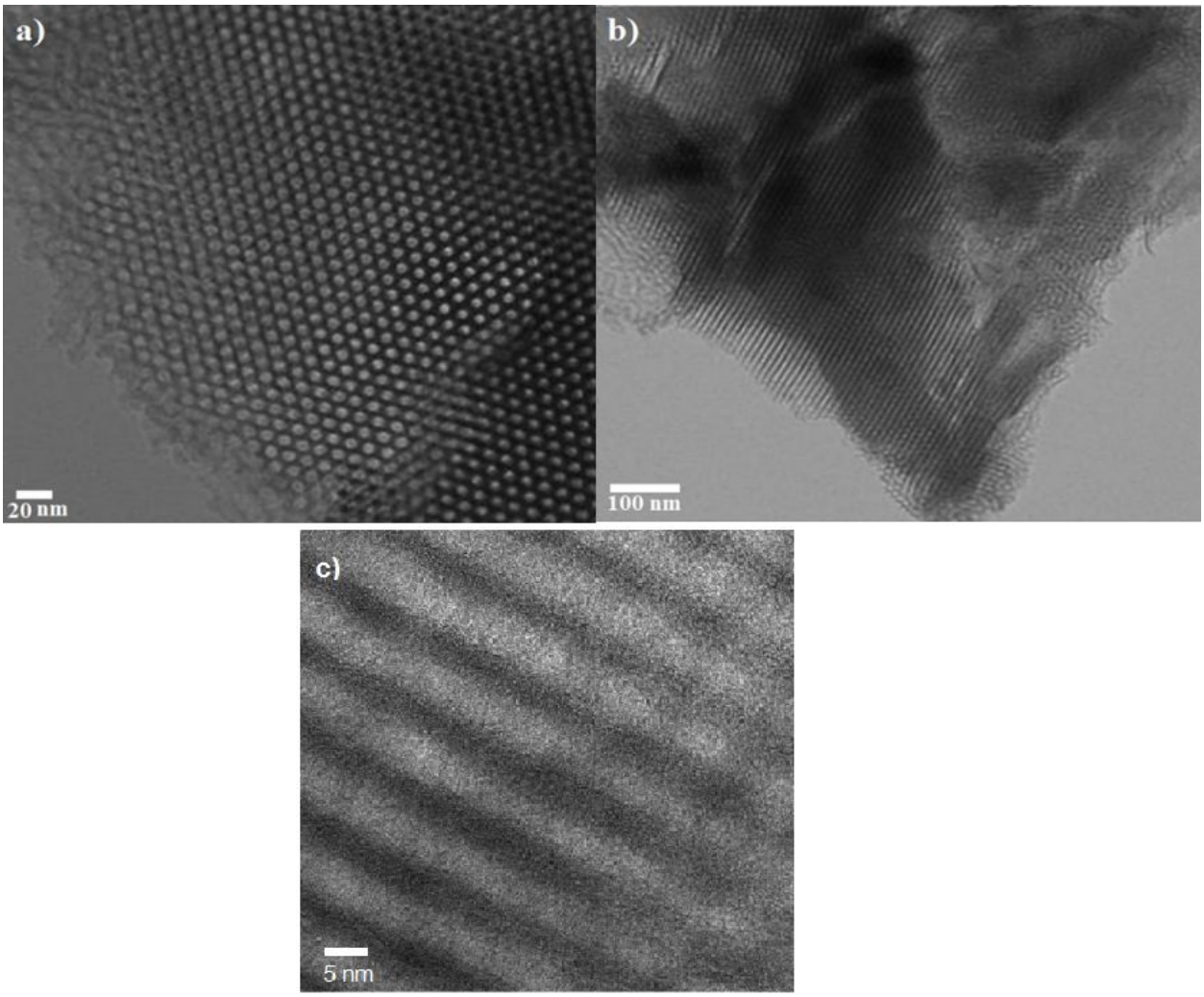

Figure 2. TEM images of PMO-IL (a) and Au@PMO-IL (b and c)

The integrity of organic groups inside the PMO-IL channels was also examined by diffuse reflectance infrared Fourier transform spectroscopy (DRIFT). Both materials displayed similar patterns and peak intensity (Figures S1-S2). The peaks observed at ca. 950 and 1100 cm^{-1}, can be assigned to asymmetric and symmetric stretching vibrations of Si-O-Si bonds.[60] In addition the vibration around 2950 cm^{-1} corresponds to the asymmetric stretching vibration of aliphatic or C-H bonds in the bridged imidazolium units.[61] Moreover, the presence of imidazolium moieties may be further confirmed by the vibration at 1633 cm^{-1} which is related to the stretching vibration of C=N bonds.[62] Peaks at 800 and 3440 cm^{-1} can be attributed to bending vibrations of Si-C bonds and stretching vibration of O-H in surface silanol groups, respectively.[50] These results indicate that PMO precursors well incorporated during the *Sol-Gel* process, and retained during the aging, surfactant extraction stage and catalyst preparation through ion exchanging process.

The thermal stability as well as organic content of catalyst was evaluated by thermogravimetric analysis (TGA) in temperatures ranging from 20 to 800 °C under air flow (Figure 3). The first stage (ca. 6 wt%) occurring below 150 °C may be due to desorption of solvent molecules that remained from either solvent-extraction processes or during catalyst preparation stages. The subsequent main mass-loss of ca. 21 wt% between 350 and 600 °C is most likely related to the decomposition of the bridged imidazolium ionic liquids in the framework of catalyst. From the last data, the amounts of ionic liquid were approximately determined to be 1.1 $mmol.g^{-1}$. Finally, the gold contents in the catalyst were found to be 0.09 mmol g-1 using inductively coupled plasma atomic emission spectroscopy (ICP-AES) from its acid washed solution.

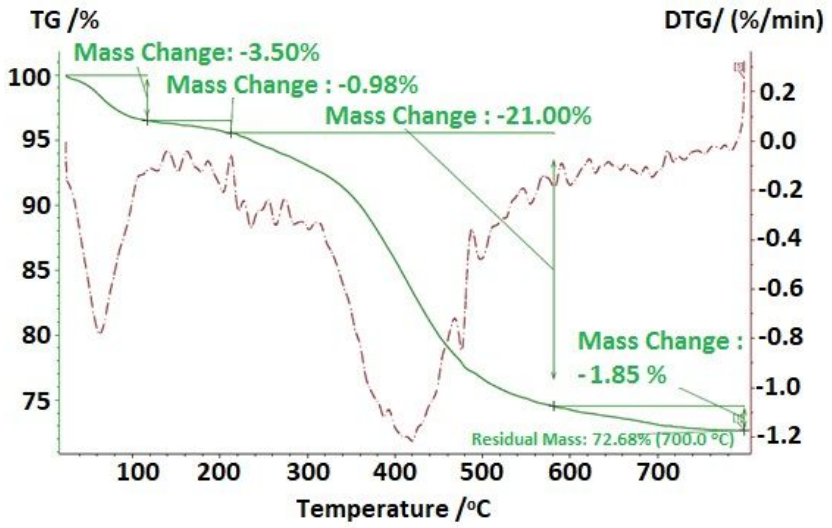

Figure 3. TG pattern for Au@PMO-IL

Once the final catalyst was characterized, its activity was first evaluated as recoverable catalyst for the aerobic oxidation of alcohols under a normal pressure of molecular oxygen and at the ambient temperature. The aerobic oxidation of benzyl alcohol (0.5 mmol) was first tested in various solvents, catalyst loadings, and in the presence of Cs_2CO_3 following to our previous successful experience of using this base in the gold-catalyzed aerobic oxidation of alcohols to find the best optimized reaction conditions (Table 2).[63] Our studies revealed that Cs_2CO_3 with combination of toluene gave the best result as compared with the other solvents like CH_3CN:H_2O, CH_3CN, H_2O, CH_2Cl_2 and α,α,α-trifluorotoluene (TFT) (Table 2, entry 6 vs. entries 1-5). Here we attribute the high catalytic activity of Au@PMO-IL in toluene to superior solubility of molecular oxygen in this solvent, a feature which is in good agreement to our previous reports.[64-66] In the next stage, the activity of catalyst was also probed in the presence of various bases in the toluene as solvent in the same reaction. In this regard, several bases such as Et_3N, Na_2CO_3, K_2CO_3 and $CaCO_3$ were also examined, but all of them resulted in poor yields of benzaldehyde (Table 2,

entries 7-9). Although, all carbonate bases have relatively the same basicity, either the higher solubility of Cs_2CO_3 at lower temperature in a nonpolar solvent as toluene or a phenomena so-called "Cesium effect" might be to some extent the reasons for superior activity observed in the case of using Cs_2CO_3 as exogenous base.[67,68] The initial experiments using K_2CO_3 gave 88% conversion after 12 h, under otherwise the same reaction conditions, but it was impossible to obtain complete conversion even after prolonged reaction times (48h) (Table 1, entry 10). While decreasing the catalyst loading from 0.4 to either 0.2 or 0.1 mol% did not apparently affect the overall efficiency of the process in the case of using benzyl alcohol (Table 1, entries 11 and 12), these conditions were proved to be significantly less efficient for oxidation of other alcohols. Therefore, the best conditions were found to be alcohol (0.5 mmol), Au@PMO-IL (0.4 mol%), Cs_2CO_3 (1.5 mmol), O_2 (1 atm.) in toluene (0.7 mL) at 35 °C during 3.5 h (Table 2, entry 6).

Table 2. Effects of solvents, catalyst loadings and bases in the aerobic oxidation of benzyl alcohol catalyzed by Au@PMO-IL.[a]

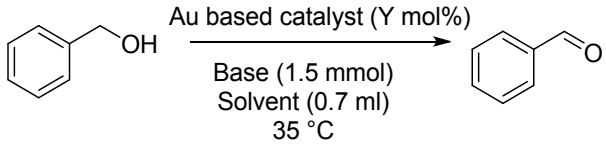

Entry	Catalyst (Y)	Solvent	Base	t (h)	Con.[b] (%)	Sel. [c] (%)	TON[d]
1	Au@PMO-IL (0.4)	$CH_3CN:H_2O$	Cs_2CO_3	24	5	>99	12.5
2	Au@PMO-IL (0.4)	CH_3CN	Cs_2CO_3	24	8	>99	20
3	Au@PMO-IL (0.4)	H_2O	Cs_2CO_3	24	11	93	27.5
4	Au@PMO-IL (0.4)	CH_2Cl_2	Cs_2CO_3	12	83	>99	207.5
5	Au@PMO-IL (0.4)	TFT	Cs_2CO_3	8	90	>99	225

6	**Au@PMO-IL (0.4)**	**Toluene**	**Cs_2CO_3**	**3.5**	**>99**	**>99**	**250**
7	Au@PMO-IL (0.4)	Toluene	Et_3N	24	25	>99	62.5
8	Au@PMO-IL (0.4)	Toluene	Na_2CO_3	24	10	>99	25
9	Au@PMO-IL (0.4)	Toluene	$CaCO_3$	24	25	>99	62.5
10	Au@PMO-IL (0.4)	Toluene	K_2CO_3	12	88	>99	220
11	Au@PMO-IL (0.2)	Toluene	Cs_2CO_3	6	97	>99	242.5
12	Au@PMO-IL (0.1)	Toluene	Cs_2CO_3	12	85	>99	212.5
13	Au-Catalyst-(**1**) (0.4)	Toluene	Cs_2CO_3	6	98	>99	245
14	Au-Catalyst-(**1**) (0.4)	Toluene	K_2CO_3	24	37	>99	92.5
15	Au-Catalyst-(**2**) (0.4)	Toluene	Cs_2CO_3	24	10	>99	25
16[e]	Au@SBA-15 (0.4)	Toluene	Cs_2CO_3	24	<5	>99	12.5

[a] Reaction conditions: benzyl alcohol (0.5 mmol), catalyst (0.1-0.4 mol%, 5-20 mg), solvent (0.7 ml), base (1.5 mmol), O_2 (1atm.) at 35 °C. [b] GC yields using internal standard method. [c] Reaction selectivity to benzaldehyde. [d] Turn over frequency, TON = $\frac{yield(\%)}{Cat.\ (mol\,\%)}$. [e] Au@SBA-15 was prepared according to our literature procedure.[49] Although due to some limitations the reactivity differences have been compared in all data at the high end conversions, a more realistic comparison could be achieved at lower initial conversion.

In the next stage, the influence of the preparation method on the catalytic performance of our catalyst was also studied in oxidation of benzyl alcohol under optimized conditions (Table 2, entry 13-16). To do this, Au-catalyst-(1) and Au-catalyst-(2) with the same metal loading were prepared via impregnation followed by reduction of Au(III) species by employing $NaBH_4$ (for catalyst 1) and benzyl alcohol (for catalyst 2) as reducing agents, respectively (see Experimental Section for details). Although, Au-catalyst-(1) showed also remarkable catalytic activity for oxidation of benzyl alcohol (Table 2, entry 13), the activity was dramatically declined in the case of oxidation of non-activated and hindered alcohols which often need much longer reaction time (Table S2). This suggests that pre-generated Au nanoparticles could not provide durable catalytic activity most

likely because of their agglomeration and subsequent deactivation. On the other hand, Au-catalyst-(2) prepared via benzyl alcohol reduction protocol, showed poor activity and only generated benzaldehyde in 10% yields after 24 h (Table 2, entry 15). Therefore, the much higher as well as durable activity of our Au@PMO-IL as compared to Au-catalyst-(1) and -(2) may be also attributed to the different Au composition on the surface of these materials. We will discuss this issue later in the manuscript. It is also worth noting that a catalyst prepared by immobilization of $NaAuCl_4$ on SBA-15 showed very poor activity in the aerobic oxidation of benzyl alcohol (Table 2, entry 16). This finding clearly demonstrates that presence of imidazolium groups in the interior of PMO channels can provide efficient environment for both excellent distributions of AuNPs and their long term stabilization.[58]

With the optimal reaction conditions in hand, we then evaluated the generality of the catalytic system in aerobic oxidation of various primary, secondary, and even sterically hindered alcohols (Table 3). A wide range of primary or secondary benzylic alcohols comprising either electron withdrawing, releasing group or sterically hindrances were converted to the corresponding carbonyl compounds in excellent yields and superior selectivity (Table 3, entries 1-16). Selective oxidation of linear primary aliphatic alcohols catalyzed by gold catalysts, regarded as a highly challenging process at room temperature. Although, somewhat higher catalyst loading was needed, 3-phenyl propanol and n-heptanol were selectively oxidized to the related aldehyde within 24h at room temperature in excellent yields and selectivity, (Table 3, entries 11-12).

The alcohols comprising heteroatoms, also considered as another highly challenging substrates for aerobic oxidation in the most transition-metal catalyst systems because the strong coordination of these alcohols to metal center deactivates the catalyst. However, we found that some related

alcohols can convert to the expected aldehyde in moderate to good yield and excellent selectivity (Table 3, entries 17-20).

While many reports are concerned to the gold-catalyzed oxidation of primary alcohols to the corresponding aldehydes, the oxidation of secondary aliphatic alcohols to the corresponding ketones has been less studied. Using the present procedure, Au@PMO-IL also showed excellent activity for the selective oxidation of open chain secondary aliphatic alcohols at room temperature (Table 3, entry 24). In particular, under the optimized reaction conditions, alcohols with sensitive functional groups such as propargylic and c-propyl moieties afforded the corresponding ketones in excellent yields and selectivity without any detectable side-products (Table 3, entries 25–26). Interestingly, the oxidation of cyclic aliphatic alcohols under the same reaction conditions furnished the expected ketones in good to excellent yields (Table 3, entries 27–32). However, the oxidation of borneol and menthol only produced moderate yields of the corresponding ketones (Table 3, entries 33 and 34). To the best of our knowledge, oxidation of such highly encumbered alcohols in the presence of gold catalyst at room temperature has not yet been reported.

Table 3. Aerobic oxidation of alcohol catalyzed by Au@PMO-IL in the presence of Cs_2CO_3.[a]

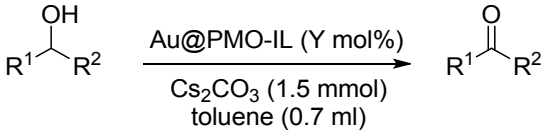

Entry	R^1	R^2	Y	t (h)	Con.[b] (%)	Sel. [c] (%)	TON[d]
1	C_6H_5	H	0.4	3.5	>99	>99	250
2	4-CH_3-C_6H_4	H	0.4	6	>99	>99	250
3	4-CH_3O-C_6H_4	H	0.4	3	>99	>99	250

4	4-*i*-C_3H_7-C_6H_4	H	0.4	12	>99	>99	250
5	4-Cl-C_6H_4	H	0.4	12	>99	>99	250
6	4-NO_2-C_6H_4	H	0.4	20	>99	>99	250
7	2-CH_3-C_6H_4	H	0.4	7	>99	>99	250
8	2-NO_2-C_6H_4	H	0.4	16	>99	>99	250
9	3-Cl-C_6H_4	H	0.4	8	>99	>99	250
10	2,4-*di*-Cl-C_6H_3	H	0.4	16	>99	>99	250
11	$C_6H_5CH_2CH_2$	H	2	24	>99	>99	50
12	*n*-C_6H_{13}	H	5	24	95	>99	19
13	$(CH_3)_2C=CH$	H	2	30	75	>99	36
14	C_6H_5	C_6H_5	0.4	5	>99	>99	250
15	C_6H_5	CO C_6H_5	0.4	7	>99	>99	250
16	4-Cl-C_6H_4	CO C_6H_4-4-Cl	0.4	24	95	>99	238
17	4-CH_3S-C_6H_4	H	2	48	96	>99	48
18[e]	2-Furyl	H	2	12	65	>99	32
19[e]	3-Pyridyl	H	2	4	45	>99	22
20[e]	3-Pyridyl	CH_3	2	24	50	>99	24
21	*n*-C_5H_{11}	CH_3	0.4	7	97	>99	242
22	$C_6H_5CH_2CH_2$	CH_3	0.4	12	95	>99	238
23	*c*-C_6H_{13}	CH_3	0.4	12	95	>99	238
24	*c*-C_6H_{11}	C_6H_4	0.4	12	>99	>99	250
25	*c*-C_3H_5	*c*-C_3H_5	0.4	12	80	>99	200
26	*n*-C_5H_{11}	C≡CH	2	24	80	>99	41
27	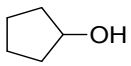		2	24	95	>99	46
28	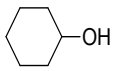		2	24	95	>99	46

29	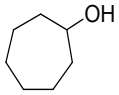	0.4	8	>99	>99	250
30	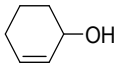	2	8	75	>99	37
31	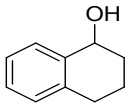	0.4	4	>99	>99	250
32	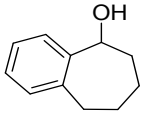	0.4	10	>99	>99	250
33	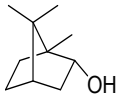	2	24	45	>99	22
34	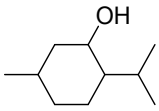	2	24	20	>99	10

[a] Reaction conditions: alcohol (0.5 mmol), catalyst (0.4-5 mol%), toluene (0.7 ml), Cs_2CO_3 (1.5 mmol), O_2 (1atm.) at 35 °C unless otherwise stated. [b] GC yields using internal standard method. [c] Reaction selectivity to desired product. [d] TON = $\frac{yield(\%)}{Cat.(\,mol\,\%))}$. [e] TFT was used as solvent.

To gain a better insight into the nature of the Au species in the Au@PMO-IL and more importantly the significant difference between various Au catalysts investigated in this study, a thin film of the materials was prepared and analyzed using X-Ray photoelectron spectroscopy (XPS). Figure 4 displays the XPS spectra of the catalysts prepared by the different methods in the binding energy range for Au4f signals. The XPS spectra for Au-Catalyst-(1) and Au@PMO-IL show only peaks located at 85-88 and 87-90 eV, respectively. These peaks assigned to the spin–orbit split components of the $Au^{(0)}4f_{7/2}/Au^{(0)}4f_{5/2}$ and $Au^{(3+)}\ 4f_{7/2}/Au^{(3+)}4f_{5/2}$ levels in the materials, respectively (Figure 4).[58] The spectra of the fresh Au@PMO-IL mainly contain $Au^{(3+)}$ as indicated by intense peaks at 86.5 and 90.5 eV. In contrary, the XPS spectrum of Au-catalyst-(1) only contains peaks at 84.7 and 88.4 and a spin-orbit splitting of ~3.7 eV representing gold in metallic

form $Au^{(0)}$. In this regard, apparently $Au^{(3+)}$ ions play a crucial role in enhancement of catalytic activity. Therefore, the much higher activity of Au@PMO-IL as compared to Au-catalyst-(1) might be attributed to higher $Au^{(3+)}/Au^{(0)}$ ratios on the surface of the materials. It is speculated that in the case of Au@PMO-IL, $Au^{(3+)}$ species may act as Lewis acid and coordinated with substrate, a feature allowing starting alcohols to present in the nanospaces of the catalyst in high concentration, where they can more efficiently oxidize at available Au active sites.

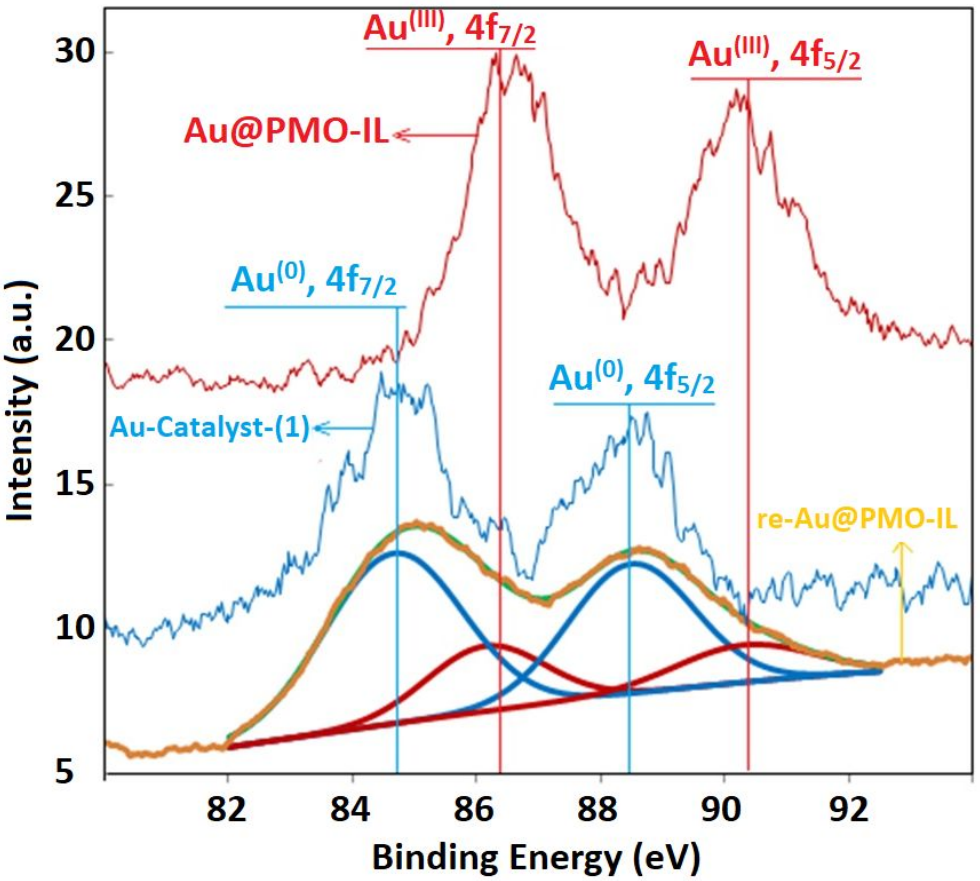

Figure 4. XPS spectra for Au@PMO-IL (red line) Au-catalysts-(**1**) (blue line) and recovered Au@PMO-IL (yellow line).

In the next stage, we were very interested to study the scope of present catalytic system by employing K_2CO_3 as a cheaper base than Cs_2CO_3 (Table 4, entries 1–7). As it was already pointed

out before in the manuscript, in the presence of K_2CO_3, toluene and 0.4 mol % of Au@OMO-IL, benzyl alcohol was efficiently converted to benzaldehyde in good yields of 88% at 35 °C (Table 2, entry 10). However, the reaction was not completed even after prolonged (24 h) reaction times. Our preliminary investigations also showed that this condition was not suitable for the efficient oxidation of other alcohols. With the aim to optimum reaction conditions, several parameters were checked and it was found that the use of K_2CO_3 (1.5 mmol), catalyst Au@PMO-IL (0.2 mol%), toluene as solvent at 60 °C, are the best conditions for this catalytic system (Table 4, entry 5).

Table 4. Effects of solvents, catalyst loadings and temperature in the aerobic oxidation of benzyl alcohol catalyzed by Au@PMO-IL in the presence of K_2CO_3. [a]

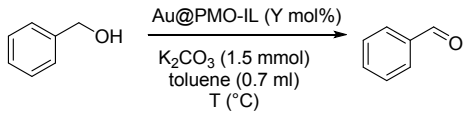

Entry	Y	T (°C)	Time(h)	Con.[b] (%)	Sel. [c] (%)	TON[d]
1	0.4	35	12	88	>99	95
2	0.1	60	12	38	>99	378
3	0.1	70	12	54	>99	540
4	0.1	80	6	89	>99	990
5	**0.2**	**60**	**6**	**>99**	>99	500
6	0.2	70	6	>99	>99	500
7	0.2	80	5	>99	>99	500

[a] Reaction conditions: benzyl alcohol (0.25 mmol), catalyst (0.4 mol%), toluene (0.7 ml), K_2CO_3 (1.5 m0mol), O_2 (1atm.) [b] GC yields using internal standard method. [c] Reaction selectivity to benzaldehyde. [d] TON = $\frac{yield(\%)}{Cat.\ (mol\%)}$

Interestingly, under the same reaction conditions, various benzylic alcohols gave the respective benzaldehyde in high yields and selectivities (Table 5, entries 1-12). Even in the case of more challenging aliphatic alcohols, the corresponding aldehydes were obtained in excellent yields and

selectivities (Table 5, entries 13 and 14). The oxidation of cinnamyl alcohol, gave cinnamaldehyde in excellent yields and selectivity without the formation of any detectable side products (Table 5, entry 15). However, the oxidation of 3-methyl-2-buten-1-ol only produced moderate yields of the corresponding aldehyde even in the presence of relatively 1 mol% of Au@PMO-IL (Table 5, entry 16). The alcohols bearing heteroatoms were also oxidized to furnish the expected carbonyl compounds in moderate to excellent yields (Table 5, entries 17-20). It is also worth mentioning that under essentially identical reaction conditions, various linear secondary aliphatic alcohols were easily converted to the corresponding ketones in good to excellent yields (Table 5, entries 21-29). However, in the case of dicyclopropylmethanol and 1-octyn-3-ol somewhat higher catalyst loadings were needed to obtain acceptable yield of the corresponding ketones (Table 5, entries 30 and 31). Some activated and non-activated cyclic secondary alcohols could also be converted to the related ketones in excellent yields (Table 5, entries 32-37). Unfortunately, menthol and borneol were oxidized in the moderate yields even after prolonged reaction times in the presence of 5 mol% of catalyst (Table 5, entries 38-39).

Table 5. Aerobic oxidation of alcohol catalyzed by Au@PMO-IL in the presence of K_2CO_3. [a]

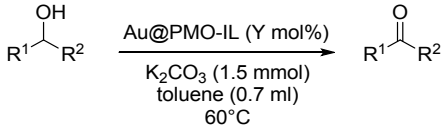

Entry	R^1	R^2	Y	t (h)	Con.[b] %)	Sel.[c] (%)	TON[d]
1	C_6H_5	H	0.2	6	>99	>99	500
2	4-CH_3-C_6H_4	H	0.2	7	>99	>99	500
3	4-CH_3O-C_6H_4	H	0.2	4	>99	>99	500
4	4-*i*-C_3H_7-C_6H_4	H	0.2	16	>99	>99	500

5	4-Cl-C_6H_4	H	0.2	24	>99	>99	500
6	4-Br-C_6H_4	H	0.2	24	95	>99	475
7	4-NO_2-C_6H_4	H	0.2	20	>99	>99	500
8	2-CH_3-C_6H_4	H	0.2	12	>99	>99	500
9	2-NO_2-C_6H_4	H	0.2	24	>99	>99	500
10	3-Cl-C_6H_4	H	0.2	14	>99	>99	500
11	3-Br-C_6H_4	H	0.2	30	>99	>99	500
12	2,4-*di*-Cl-C_6H_3	H	0.2	24	>99	>99	500
13	$C_6H_5CH_2CH_2$	H	1	30	>99	>99	99
14[e]	*n*-C_6H_{13}	H	5	24	95	>99	19
15	$C_6H_5CH=CH$	H	0.2	7	>99	>99	500
16	$(CH_3)_2C=CH$	H	1	24	10	>99	10
17	4-CH_3S-C_6H_4	H	2	24	75	>99	36
18[f]	2-Furyl	H	2	24	65	>99	31
19[f]	3-Pyridyl	H	2	30	45	>99	21
20[f]	3-Pyridyl	CH_3	2	30	50	>99	24
21	*n*-C_5H_{11}	CH_3	0.2	30	97	>99	483
22	C_6H_5	CH_3	0.2	12	>99	>99	500
23	C_6H_5	C_2H_5	0.2	14	>99	>99	500
24	C_6H_5	C_6H_5	0.2	4	>99	>99	500
25	C_6H_5	CO C_6H_5	0.2	8	>99	>99	500
26	4-Cl-C_6H_4	CO C_6H_4-4-Cl	0.2	30	95	>99	474
27	$C_6H_5CH_2CH_2$	CH_3	0.2	24	95	>99	475
28	$_c$-C_6H_{13}	CH_3	0.2	24	>99	>99	500
29	*c*-C_6H_{11}	C_6H_5	0.2	14	>99	>99	500
30	*c*-C_3H_5	*c*-C_3H_5	1	14	80	>99	80

31	*n*-C_5H_{11}	C≡CH	1	48	45	>99	43
32		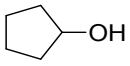	0.2	20	95	>99	474
33		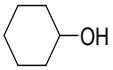	1	24	95	>99	94
34		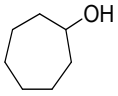	0.2	14	>99	>99	500
35		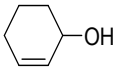	1	24	75	>99	74
36		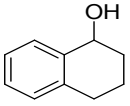	0.2	4	>99	>99	500
37		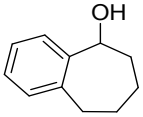	0.2	12	>99	>99	500
38[e]		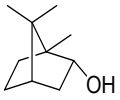	5	24	45	>99	7
39[e]		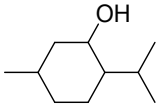	5	24	30	>99	5

[a] Reaction conditions: alcohol (0.25 mmol), catalyst (0.4-5 mol%), toluene (0.7 ml), K_2CO_3 (1.5 mmol), O_2 (1atm.) at 35 °C unless otherwise stated. [b] Conversion of alcohols determined by GC using internal standard method. [c] Reaction selectivity to benzaldehyde. [d] TON = $\frac{yield(\%)}{Cat.\,(mol\%))}$. [e] At 80 °C. [f] TFT was used as solvent.

When using a heterogeneous catalyst, the questions regarding the reuse and the leaching of active species in solution should be resolved. Therefore, it is very important to determine whether or not support itself survives the reaction conditions and the actual catalysis was from leached or supported metal. In this regard, the recycling of Au@PMO-IL was assessed in the aerobic oxidation of benzyl alcohols under described reaction conditions in entry 6 of Table 2. After first run, the catalyst was recovered by simple filtration, followed by washing with excess amount of

water and acetone, and dried under vacuum. The recovered catalyst was then reused for the next run, as shown in Figure S10, the catalyst still shows good activity and excellent selectivity over seven consecutive reactions. A filtration test at 35 °C showed that no soluble Au was detected using ICP-AES within the detection limit (0.2 ppm). Moreover, the ICP-AES analysis indicated that the Au contents in the catalyst after 7th catalytic cycle remained unchanged (0.085 mmol g^{-1}). We also conducted a filtration test for oxidation of benzyl alcohol catalyzed by Au@PMO-IL in the presence of cesium carbonate (Cs_2CO_3) as base. In this regard, the aerobic oxidation of benzyl alcohol was initially carried out under optimized reaction (1.5h, 45%) [See the Experimental Sections for details]. We found that the reaction did not carefully progress and benzaldehyde was obtained in only 2%. These findings clearly demonstrate that alkyl imidazolium groups in the interior of mesochannels of Au@PMO-IL not only serve as a handle for in situ generation and stabilization of gold nanoparticles but they can also effectively prevent the leaching of Au species into solution during the reaction process. In addition to investigating the loss of Au from the catalyst upon treatment under reaction condition, the structural integrity of catalyst was assessed in several ways. Nitrogen adsorption-desorption isotherm of the recovered Au@PMO-IL showed a type IV isotherm with a narrow hysteresis loop which confirms structural order of Au@PMO-IL largely retained during reaction process (Figure 1, S11). In comparison to fresh catalyst, the BET surface area and mesoporous volume for recovered catalyst were decreased from 432 and 0.77 to 355 m^2 g^{-1} and 0.58 cm^3 g^{-1}, respectively (Table 1). Interestingly, BJH calculations revealed a relatively sharp pore size distribution centered around 9.2 nm similar to fresh catalyst (Figure 1, S12). These findings clearly demonstrate that structural ordering of catalyst significantly remained intact under basic reaction conditions. However, it should be noted a relatively two-stage desorption in N_2 adsorption-desorption isotherm of the recovered Au@PMO-IL observed which

is very similar to those of mesoporous silica/organosilica with confinement channels so called plugged hexagonal templated silica (PHTS) materials.[69] Such adsorption-desorption isotherm is very similar to those materials having both open and plugged (constricted) cylindrical mesopores. As we have already explained and by providing several compelling evidences including TEM miscroscopy of both fresh and recycled Au@PMO-IL (See Figure 5), Au nanoparticles are produced both inside and outside the mesochannels of PMO-IL during the catalytic process. Therefore, it is most likely that the generated Au nanoparticles inside the mesochannels could behave as "plugs" in some mesopores. In this case, open pores are gradually desorbed at reduced relative pressures in a normal way but blocked pores with AuNPs will remain filled until the vapor pressure is lowered to $P/P_0 = 0.45$ (lower limit for Hysteresis P/P_0) when condensed N_2 eventually desorbs.[70]

Transmission electron microscopy (TEM) image of recovered Au@PMO-IL after the seventh reaction cycle not only proved the retention of ordered structure in the catalyst after reaction and recovery, but also confirm that agglomeration of Au nanoparticles was negligible during reaction processes and recycling (Figure 5). Finally, TG diagram of the recovered catalyst showed weight-loss of ca. 25% between 350 and 600 °C (Figure S13). This observation also indicated that bridged imidazolium ionic liquids in the catalyst framework remained intact under basic reaction conditions. Interestingly, the XPS spectrum of the recovered catalyst Au@PMO-IL confirmed the presence of both $Au^{(3+)}$ and $Au^{(0)}$ species in the reused catalyst, which highlights the notion that the $Au^{(III)}$ species remain on the surface of Au in metallic form even in the recycled catalyst (Figure 4).

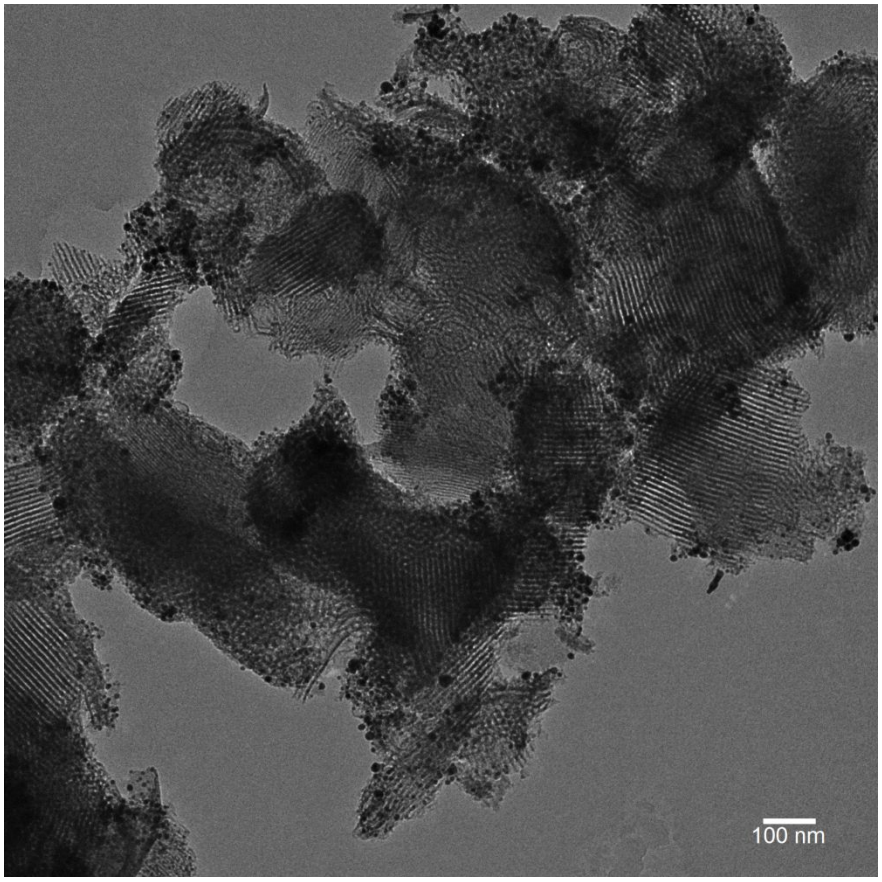

Figure 5. TEM image of recovered Au@PMO-IL catalyst after 7th run in the oxidation of benzyl alcohol

Conclusion

In conclusion, among three distinct Au supported catalysts onto periodic mesoporous organosilica with imidazolium framework (PMO-IL), *in situ* generated gold nanoparticles inside the nanospaces of PMO-IL (Au@PMO-IL) exhibits superior activity, selectivity and high stability as well as good reusability in the aerobic oxidation of activated and non-activated alcohols in the presence of either Cs_2CO_3 (35 °C) or K_2CO_3 (60 °C) as reaction bases under mild reaction conditions. It was found that the activity is strongly influenced by the method of generating the

Au nanoparticles inside the well-ordered mesopore networks of PMO-IL. Our studies imply that the co-existence of $Au^{(3+)}$ ions and $Au^{(0)}$ on the surface of catalyst play a crucial role in enhancement of catalytic activity. This is most likely explained by the fact that high local $Au^{(3+)}$ concentration of the surface of catalyst act as Lewis acid and coordinated with substrate, a feature allowing starting alcohols to present in the nanospaces of the catalyst in high concentration, where they can more efficiently oxidize at available Au active sites before they can release back to the solution. The amounts of leached catalyst were very negligible (<0.2 ppm) and catalyst was recovered at least seven reaction cycles. High stability and reusability catalyst can be attributed to the presence of ionic liquid in the catalyst, a finding that is in good agreement with reference catalyst experiment and structural analysis of a sample of recovered catalyst.

ASSOCIATED CONTENT

Supporting Information including reaction procedures, additional characterization and spectroscopic data for products is available.

AUTHOR INFORMATION

Corresponding Author

* Babak Karimi, 0000-0002-0453-0047

† Department of Chemistry, Institute for Advanced Studies in Basic Sciences (IASBS),

No. 444, Prof. Yousef Sobouti Blvd., Zanjan 45137-66731, Iran.

Email: karimi@iasbs.ac.ir; Fax: +98-24-3341-4747; Tel: +98-24-3315-3225

‡ Research Center for Basic Sciences & Modern Technologies (RBST), Institute for Advanced Studies in Basic Sciences (IASBS), Zanjan 45137-66731, Iran

ACKNOWLEDGMENT

The authors acknowledge IASBS Research Councils (Grant no. G2019IASBS31100), and Iranian National Science Foundation (INSF, Grant no. G020), NanoQuebec and Natural Sciences and Engineering Research Council of Canada (H.V.) for support of this work.

Reference

(1) Hudlicky, M. *Oxidation in Organic Chemistry*, ACS Monograph Series, American Chemical Society, Washington, DC, **1990**.

(2) Ley, S. V.; Madfin, A. *Comprehensive organic synthesis* Eds. Trost, B. M.; Fleming, I. Vol 7 Oxidation, Pergamon Press, Oxford UK, **1991**, pp 251–289.

(3) Cole-Hamilton, D. J. Homogeneous Catalysis-New Approaches to Catalyst Separation, Recovery, and Recycling, *Science* **2003**, *299*, 1702-1706.

(4) Geletii, Y. V.; Botar, B.; Koegerler, P.; Hillesheim, D. A.; Musaev, D. G.; Hill, C. L.; An All-Inorganic, Stable, and Highly Active Tetraruthenium Homogeneous Catalyst for Water Oxidation, *Angew. Chem., Int. Ed*. **2008**, *47*, 3896-3899.

(5) Diez-Gonzalez, S.; Marion, N.; Nolan, S. P. N-Heterocyclic Carbenes in Late Transition Metal Catalysis, *Chem. Rev*. **2009**, *109*, 3612-3676.

(6) Gorin, D. J.; Sherry, B. D.; Toste, F. D. Ligand Effects in Homogeneous Au Catalysis, *Chem. Rev*. **2008**, *108*, 3351-3378.

(7) Li, R.; Zhang, P.; Huang, Y.; Zhang, P.; Zhong, H.; Chen, Q. Pd–Fe_3O_4@C Hybrid Nanoparticles: Preparation, Characterization, and Their High Catalytic Activity Toward Suzuki Coupling Reactions, *J. Mater. Chem.* **2012**, *22*, 22750-22755.

(8) Caron, S.; Dugger, R. W.; Ruggeri, S. G.; Ragan, H. A.; Ripin, D. H. B. Large-Scale Oxidations in the Pharmaceutical Industry, *Chem. Rev*. **2006**, *106*, 2943-2989.

(9) Allen, S. E.; Walvoord, R. R.; Padilla-Salinas, R.; Kozlowski, M. C. Aerobic Copper-Catalyzed Organic Reactions, *Chem. Rev*. **2013**, *113*, 6234-6458.

(10) Xue, Z.; Zhang, J.; Peng, L.; Han, B.; Zhang, T.; Li, J.; Yang, Y. Poly(ethylene glycol) Stabilized Mesoporous Metal–Organic Framework Nanocrystals: Efficient and Durable Catalysts for the Oxidation of Benzyl Alcohol, *ChemPhysChem* **2013**, *15*, 85-89.

(11) Chen, J.; Zhang, Q.; Wang, Y.; Wan, H. Size-Dependent Catalytic Activity of Supported Palladium Nanoparticles for Aerobic Oxidation of Alcohols, *Adv. Synth. Catal*. **2008**, *350*, 453-464.

(12) Slot, T. K.; Eisenberg, D.; van Noordenne, D.; Jungbacker, P.; Rothenberg, G. Cooperative Catalysis for Selective Alcohol Oxidation with Molecular Oxygen, *Chem. Eur. J*. **2016**, *22*, 12307-12311.

(13) Gunasekaran, N. Aerobic Oxidation Catalysis with Air or Molecular Oxygen and Ionic Liquids, *Adv. Synth. Catal*. **2015**, *357*, 1990-2010.

(14) Sangtrirutnugul, P.; Chaiprasert, T.; Hunsiri, W.; Jitjaroendee, T.; Songkhum, P.; Laohhasurayotin, K.; Osotchan, T.; Ervithayasuporn, V. Tunable Porosity of Cross-Linked-

Polyhedral Oligomeric Silsesquioxane Supports for Palladium-Catalyzed Aerobic Alcohol Oxidation in Water, *ACS Appl. Mater. Interfaces* **2017**, *9*, 12812-12822.

(15) Yao, X.; Bai, C.; Chen, J.; Li, Y. Efficient and Selective Green Oxidation of Alcohols by MOF-derived Magnetic Nanoparticles as a Recoverable Catalyst, *RSC Adv*. **2016**, *6*, 26921-26928.

(16) Davis, S. E.; Ide, M. S.; Davis, R. J. Selective Oxidation of Alcohols and Aldehydes Over Supported Metal, *Green Chem*. **2013**, *15*, 17-45.

(17) Bai, C.; Li, A.; Yao, X.; Liu, H.; Li, Y. Efficient and Selective Aerobic Oxidation of Alcohols Catalysed by MOF-derived Co Catalysts, *Green Chem*. **2016**, *18*, 1061-1069.

(18) Bai, L.; Zhang, S. Chen, Q.; Gao, C. Synthesis of Ultrasmall Platinum Nanoparticles on Polymer Nanoshells for Size-Dependent Catalytic Oxidation Reactions, *ACS Appl. Mater. Interfaces* **2017**, *9*, 9710-9717.

(19) Mori, K.; Yamaguchi, K.; Hara, T.; Mizugaki, T.; Ebitani, K.; Kaneda, K. Controlled Synthesis of Hydroxyapatite-Supported Palladium Complexes as Highly Efficient Heterogeneous Catalysts, *J. Am. Chem. Soc*. **2004**, *124*, 11572-11573.

(20) Uozumi, Y.; Nakao, R.; A Well-Defined Complex for Palladium-Catalyzed Aerobic Oxidation of Alcohols: Design, Synthesis, and Mechanistic Considerations, *Angew. Chem., Int. Ed*. **2003**, *42*, 3810-3813.

(21) Mori, K.; Hara, T.; Mizugaki, T.; Ebitani, K.; Kaneda, K. Hydroxyapatite-Supported Palladium Nanoclusters: A Highly Active Heterogeneous Catalyst for Selective Oxidation of Alcohols by Use of Molecular Oxygen, *J. Am. Chem. Soc*. **2004**, *126*, 10657-10666.

(22) Hackett, S. F. J.; Brydson, R. M.; Gass, M. H.; Harvey, I.; Newman, A. D.; Wilson, K.; Lee, A. F. High-Activity, Single-Site Mesoporous Pd/Al_2O_3 Catalysts for Selective Aerobic Oxidation of Allylic Alcohols, *Angew. Chem., Int. Ed.* **2007**, *46*, 8593-8596.

(23) Parlett, C. M. A.; Bruce, D. W.; Hondow, N. S.; Newton, M. A.; Lee, A. F.; Wilson, K. Mesoporous Silicas as Versatile Supports to Tune the Palladium-Catalyzed Selective Aerobic Oxidation of Allylic Alcohols, *ChemCatChem* **2012**, *5*, 939-950.

(24) Johnston, E. V.; Verho, O.; Kärkäs, M. D.; Shakeri, M.; Tai, C. –W.; Palmgren, P.; Eriksson, K.; Oscarsson, S.; Bäckvall, J. E. Highly Dispersed Palladium Nanoparticles on Mesocellular Foam: An Efficient and Recyclable Heterogeneous Catalyst for Alcohol Oxidation, *Chem. Eur. J*. **2012**, *18*, 12202-12206.

(25) Karimi, B.; Behzadnia, H.; Bostina, M.; Vali, H. A Nano-Fibrillated Mesoporous Carbon as an Effective Support for Palladium Nanoparticles in the Aerobic Oxidation of Alcohols "on Pure Water", *Chem. Eur. J*. **2012**, *18*, 8634-8640.

(26) Yamada, Y. M. A.; Arakawa, T.; Hocke, H.; Uozumi, Y. A Nanoplatinum Catalyst for Aerobic Oxidation of Alcohols in Water, *Angew. Chem., Int. Ed*. **2007**, *46*, 704-706.

(27) Wang, T.; Xiao, C.X.; Yan, L.; Xu, L.; Luo, J.; Shou, H.; Kou, Y.; Liu, H. Aqueous-phase Aerobic Oxidation of Alcohols by Soluble Pt Nanoclusters in the Absence of Base, *Chem. Commun*. **2007**, 4375-4377.

(28) Miyamura, C.; Matsubara, R.; Kobayashi, S. Gold–platinum Bimetallic Clusters for Aerobic Oxidation of Alcohols under Ambient Conditions, *Chem. Commun*. **2008**, 2031-2033.

(29) Ng, Y. H.; Ikeda, S.; Morita, Y.; Harada, T.; Ikeue, K.; Matsumura, M. Origin of the High Activity of Porous Carbon-Coated Platinum Nanoparticles for Aerobic Oxidation of Alcohols, *J. Phys. Chem. C* **2009**, *113*, 12799-12805.

(30) Abad, A.; Concepción, C.; Corma, A.; Garcia, H. A Collaborative Effect between Gold and a Support Induces the Selective Oxidation of Alcohols, *Angew. Chem., Int. Ed*. **2005**, *44*, 4066-4069.

(31) Su, F. –Z.; Liu, Y. -M.; Wang, L. -C.; Cao, Y.; He, H. -Y.; Fan K. -N. Ga–Al Mixed-Oxide-Supported Gold Nanoparticles with Enhanced Activity for Aerobic Alcohol Oxidation, *Angew. Chem., Int. Ed*. **2008**, *47*, 334-337.

(32) Wang, X.; Kawanami, H.; Islam, N. M.; Chattergee, M.; Yokoyama, T.; Ikushima, Y. Amphiphilic Block Copolymer-stabilized Gold Nanoparticles for Aerobic Oxidation of Alcohols in Aqueous Solution, *Chem. Commun*. **2008**, 4442-4444.

(33) Miyamura, H.; Matsubara, R.; Miyazaki, Y.; Kobayashi, S. Aerobic Oxidation of Alcohols at Room Temperature and Atmospheric Conditions Catalyzed by Reusable Gold Nanoclusters Stabilized by the Benzene Rings of Polystyrene Derivatives, *Angew. Chem., Int. Ed*. **2007**, *46*, 4151-4154.

(34) Tsunoyama, H.; Sakurai, H.; Negishi, Y.; Tsukuda, T. Size-Specific Catalytic Activity of Polymer-Stabilized Gold Nanoclusters for Aerobic Alcohol Oxidation in Water, *J. Am. Chem. Soc*. **2005**, *127*, 9374-9375.

(35) Kanaoka, S.; Yagi, N.; Fukuyama, Y.; Aoshima, S.; Tsunoyama, H.; Tsukuda, T.; Sakurai, H. Thermosensitive Gold Nanoclusters Stabilized by Well-Defined Vinyl Ether Star Polymers:

Reusable and Durable Catalysts for Aerobic Alcohol Oxidation, *J. Am. Chem. Soc*. **2007**, *129,* 12060-12061.

(36) Kaizuka, K.; Miyamura, H.; Kobayashi, S. Remarkable Effect of Bimetallic Nanocluster Catalysts for Aerobic Oxidation of Alcohols: Combining Metals Changes the Activities and the Reaction Pathways to Aldehydes/Carboxylic Acids or Esters, *J. Am. Chem. Soc*. **2010**, *132*, 15096-15098.

(37) Yamaguchi, K.; Mori, K.; Mizugaki, T.; Ebitani, K.; Kaneda, K. Creation of a Monomeric Ru Species on the Surface of Hydroxyapatite as an Efficient Heterogeneous Catalyst for Aerobic Alcohol Oxidation, *J. Am. Chem. Soc*. **2000**, *122*, 7144-7145.

(38) Yamaguchi, K.; Mizuno, N.; Supported Ruthenium Catalyst for the Heterogeneous Oxidation of Alcohols with Molecular Oxygen, *Angew. Chem., Int. Ed*. **2002**, *41*, 4538-4542.

(39) Ebitani, K.; Motokura, K.; Mizugaki, T.; Kaneda, K. Heterotrimetallic RuMnMn Species on a Hydrotalcite Surface as Highly Efficient Heterogeneous Catalysts for Liquid-Phase Oxidation of Alcohols with Molecular Oxygen, *Angew. Chem., Int. Ed*. **2005**, *44*, 3423-3426.

(40) Mori, K.; Kanai, S.; Hara, T.; Mizugaki, T.; Ebitani, K.; Jitsukawa. K.; Kaneda, K. Development of Ruthenium−Hydroxyapatite-Encapsulated Superparamagnetic γ-Fe_2O_3 Nanocrystallites as an Efficient Oxidation Catalyst by Molecular Oxygen, *Chem. Mater*. **2007**, *19*, 1249-1256.

(41) Mori, S.; Takubo, M.; Makida, K.; Yanase, T.; Aoyagi, S.; Maegawa, T.; Monguchi, Y.; Sajiki, H. A Simple and Efficient Oxidation of Alcohols with Ruthenium on Carbon, *Chem. Commun*. **2009,** 5159-5161.

(42) Markó, I. E.; Giles, P. R.; Tsukazaki, M.; Brown, S. M.; Urch, C. J. Copper-Catalyzed Oxidation of Alcohols to Aldehydes and Ketones: An Efficient, Aerobic Alternative, *Science* **1996**, *274*, 2044-2046.

(43) Karimi, B.; Khorasani, M.; Vali, H.; Vargas, C.; Luque, R. Palladium Nanoparticles Supported in the Nanospaces of Imidazolium-Based Bifunctional PMOs: The Role of Plugs in Selectivity Changeover in Aerobic Oxidation of Alcohols, *ACS Catal*. **2015**, *5*, 4189-4200.

(44) Moragues, A.; Neaţu, F.; Parvulescu, V. I.; Marcos, M. D.; Amoros, P.; Michelet, V. Heterogeneous Gold Catalyst: Synthesis, Characterization, and Application in 1,4-Addition of Boronic Acids to Enones, *ACS Catal*. **2015**, *5*, 5060-5067.

(45) Haruta, M. Size- and Support-dependency in the Catalysis of Gold, *Catal. Today* **1997**, 36, 153-166.

(46) Karimi, B.; Kabiri Esfahani, K. Unexpected Golden Ullmann Reaction Catalyzed by Au Nanoparticles Supported on Periodic Mesoporous Organosilica (PMO), *Chem. Commun.* **2011**, *47*, 10452-10454.

(47) Cardona, F.; Parmeggiani, C. Transition Metal Catalysis in Aerobic Alcohol Oxidation, Chapter 5, Della Pina, C.; Fallett, E.; Rossi, M. Gold-Based Catalysis, **2015**, pp 133-154.

(48) Sharma, A. S.; Kaur, H.; Shah, D. Selective Oxidation of Alcohols by Supported Gold Nanoparticles: Recent Advances, *RSC Adv*. **2016**, *6*, 28688-28727.

(49) Karimi, B.; Kabiri Esfahani, F. Gold Nanoparticles Supported on the Periodic Mesoporous Organosilicas as Efficient and Reusable Catalyst for Room Temperature Aerobic Oxidation of Alcohols, *Adv. Synth. Catal.* **2012**, *354*, 354, 1319-1326.

(50) Karimi, B.; Elhamifar, D.; Clark, J. H.; Hunt. A. J. Ordered Mesoporous Organosilica with Ionic-Liquid Framework: An Efficient and Reusable Support for the Palladium-Catalyzed Suzuki–Miyaura Coupling Reaction in Water, *Chem. Eur. J*. **2010**, *16*, 8047-8053.

(51) Karimi, B.; Elhamifar, D.; Yari, O.; Khorasani, M.; Vali, H.; Clark, J. H.; Hunt. A. J Synthesis and Characterization of Alkyl-Imidazolium-Based Periodic Mesoporous Organosilicas: A Versatile Host for the Immobilization of Perruthenate (RuO_4^-) in the Aerobic Oxidation of Alcohols, *Chem. Eur. J*. **2012**, *18*, 13520-13530.

(52) Karimi, B.; Bakhshandeh Rostami, F.; Khorasani, M.; Elhamifar, D.; Vali, H. Selective Oxidation of Alcohols with Hydrogen Peroxide Catalyzed by Tungstate Ions ($WO_4^=$) Supported on Periodic Mesoporous Organosilica with Imidazolium Frameworks (PMO-IL), *Tetrahedron* **2014**, *70*, 6114-6119.

(53) Karimi, B.; Khorasani, M.; Bakhshandeh Rostami, F.; Elhamifar, D,; Vali, H. Tungstate Supported on Periodic Mesoporous Organosilica with Imidazolium Framework as an Efficient and Recyclable Catalyst for the Selective Oxidation of Sulfides, *ChemPlusChem* **2015**, *80*, 990-999.

(54) Gholinejad, M.; Karimi, B.; Aminianfar, A.; Khorasani, M. One-Pot Preparation of Propargylamines Catalyzed by Heterogeneous Copper Catalyst Supported on Periodic Mesoporous Organosilica with Ionic Liquid Framework, *ChemPlusChem* **2015**, *80*, 1573-1579.

(55) Karimi, B.; Naderi, Z.; Khorasani, M.; Mirzaei, H. M.; Vali, H. Ultrasmall Platinum Nanoparticles Supported Inside the Nanospaces of Periodic Mesoporous Organosilica with an Imidazolium Network: An Efficient Catalyst for the Aerobic Oxidation of Unactivated Alcohols in Water, *ChemCatChem* **2016**, *8*, 906-910.

(56) Karimi, B.; Khorasani, M.; Vali, H.; Luque, R. Control of Plugging in Bifunctional Periodic Mesoporous Organosilica with Imidazolium Framework (BFPMO) via Stepwise Addition of Silica Precursors, *J. Mater. Chem. A* **2015**, *3*, 6575-6585.

(57) Karimi, B.; Vahdati, S.; Vali, H. Synergistic Catalysis within TEMPO-functionalized Periodic Mesoporous Organosilica with Bridge Imidazolium Groups in the Aerobic Oxidation of Alcohols, *RSC Adv*. **2016**, *6*, 63717-63723.

(58) Karimi, B.; Gholinejad, M.; Khorasani, M. Highly Efficient Three-component Coupling Reaction Catalyzed by Gold Nanoparticles Supported on Periodic Mesoporous Organosilica with Ionic Liquid Framework, *Chem. Commun*. **2012**, *48*, 8961-8963.

(59) Kruk, M.; Jaroniec, M. Gas Adsorption Characterization of Ordered Organic−Inorganic Nanocomposite Materials, *Chem. Mater*. **2001**, *13*, 3169-3183.

(60) Temtsin, G.; Asefa, T.; Bittner, S.; Ozin, G. A. Aromatic PMOs: Tolyl, Xylyl and Dimethoxyphenyl Groups Integrated within the Channel Walls of Hexagonal Mesoporous Silicas, *J. Mater. Chem*. **2001**, *11,* 3202-3206.

(61) Burleigh, M. C.; Markowitz, M. A.; Spector, M. S.; Gaber, B. P. Direct Synthesis of Periodic Mesoporous Organosilicas: Functional Incorporation by Co-condensation with Organosilanes, *J. Phys. Chem. B* **2001**, *105*, 9935-9942.

(62) Karimi, B.; Enders, D. New N-Heterocyclic Carbene Palladium Complex/Ionic Liquid Matrix Immobilized on Silica: Application as Recoverable Catalyst for the Heck Reaction, *Org. Lett*. **2006**, *8*, 1237-1240.

(63) Karimi, B.; Kabiri Esfahani, F. Gold nanoparticles supported on Cs_2CO_3 as Recyclable Catalyst System for Selective Aerobic Oxidation of Alcohols at Room Temperature, *Chem. Commun*. **2009**, 5555-5557.

(64) Karimi, B.; Zamani, A.; Clark, J. H. A Bipyridyl Palladium Complex Covalently Anchored onto Silica as an Effective and Recoverable Interphase Catalyst for the Aerobic Oxidation of Alcohols, *Organometallics* **2005**, *24*, 4695-4698.

(65) Karimi, B.; Abedi, S.; Clark, J. H.; Budarin, V. Highly Efficient Aerobic Oxidation of Alcohols Using a Recoverable Catalyst: The Role of Mesoporous Channels of SBA-15 in Stabilizing Palladium Nanoparticles, *Angew. Chem., Int. Ed*. **2006**, *45*, 4776-4779.

(66) Karimi, B.; Zamani, A.; Abedi, S.; Clark, J. H. Aerobic Oxidation of Alcohols Using Various Types of Immobilized Palladium Catalyst: the Synergistic Role of Functionalized Ligands, Morphology of Support, and Solvent in Generating and Stabilizing Nanoparticles, *Green Chem*. **2009**, *11*, 109-119.

(67) Flessner, T.; Doye, S. Cesium carbonate: A powerful inorganic base in organic synthesis, *Adv. Synth. Catal.* **1999**, *341*, 186-190

(68) Ravi, V.; Kulakarni, S. R. Cesium Salts in Organic Synthesis: A Review, *Curr. Org. Chem.* **2015**, *19*, 1242-1274.

(69) Van Der Voort, P.; Ravikovitch, P. I.; De Jong, K. P.; Benjelloun, M.; Van Bavel, E.; Janssen, A. H.; Neimark, A. V.; Weckhuysen, B. M.; Vansant, E. F. A New Templated Ordered

Structure with Combined Micro- and Mesopores and Internal Silica Nanocapsules, *J. Phys. Chem. B* **2002**, *106*, 5873-5877.

(70) Groen, J. C.; Peffer, L. A. A.; Pérez-Ramírez, J. Pore size determination in modified micro- and mesoporous materials. Pitfalls and limitations in gas adsorption data analysis, *Microporous Mesoporous Mater.* **2003**, *60*, 1-17.

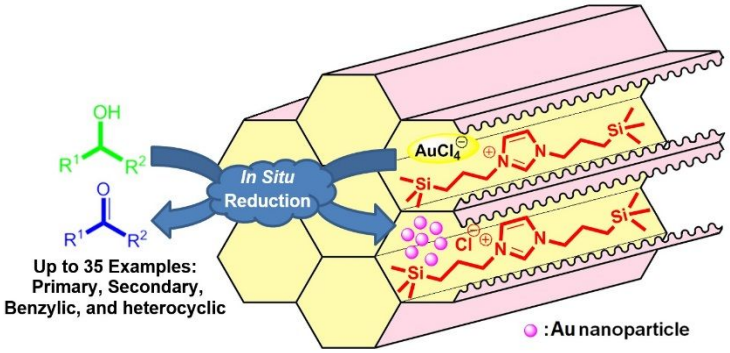

In situ generated gold nanoparticles inside the periodic mesoporous organosilica channels have been described for selective aerobic oxidation of various types of alcohols including benzylic, primary and secondary aliphatic, heterocyclic and challenging cyclic aliphatic alcohols.